Progress In Electromagnetics Research M, Vol. 109, 25–38, 2022

CB-CPW Fed SRR Loaded ISM and 5G Low Profile Antenna for On-Body Healthcare Monitor

Thangavelu Shanmuganantham[1], Srinivasan Ashok Kumar[2, *], and Dhanapalan Sindhahaiselvi[3]

Abstract—This paper explores a loaded conductor backed coplanar waveguide (CB-CPW) split ring resonator (SRR) fed U-slot planar antenna used for healthcare monitoring via the wireless scientific industrial medical (ISM) band and medical service band at fifth generation (5G-MSB). The antenna has been designed with bio-tissue layers, muscle layers, skin, and fat. The parameters of the designed antennas, such as miniaturization, increased gain, and enhanced bandwidth, are presented. The proposed prototype results in the total size of 640 mm^3. Such designed antenna has been operated at (3.4–3.6) GHz — fifth-generation medical service band and at (2.38–2.48) GHz — industrial scientific band and can realize proximately omnidirectional radiation pattern over the operating bands.

1. INTRODUCTION

Advanced wireless medical communications and other wireless network technologies like wireless LAN, WiMAX, BAN, PAN, home net, sensor networks, 5G, the recently promised to reduction of hospital delay, computer-aided scrutiny and decision making, continuous monitoring the scenario [1]. One of the best technologies for measuring ECG signal is by using metamaterial loaded with grounded coplanar feed antenna, and it enables the wireless ECG monitor for twenty-four hours. Einthoven confirmed the effective transmission of medical signal in 1906, and Shanmuganantham et al. communicated distortion ECG signal through a wireless channel in 2021 [28]. Wireless medical contact currently exists primarily in the 5G bands of medical services and ISM band. The proposed antenna worked in a higher frequency band like the ISM band of 2.36 GHz to 2.48 GHz and the fifth-generation medical service band of 5G MSB band of 3.4 GHz to 3.6 GHz in this analysis [14, 20]. Cardiovascular diseases (CVDs) are a group of disorders of the heart and blood vessels, and we need twenty-four hours continuous automatic monitoring system. The existing wired technology cannot give a good solution because it is costly and is a time consume process. The alternate solution is the ECG signal analyzed through wireless. The main advantages of these technologies have low cost and low time consumption for the monitoring.

The important characteristic of antenna design is low volume, compact with on-body, high gain, and enhanced bandwidth. The conventional design without SRR loaded structure shows low gain and bandwidth as mentioned in the results and discussion section. In 1898, J. C. Bose initiated the idea of an electromagnetic metamaterial [34]. The mathematical model was developed by Veselago et al. for negative refractive indexed materials [35]. The negative refractive index has been derived by Veselago in terms of electrical permittivity and permeability [2, 12]. The most common metamaterial structures are either circular SRR or rectangular SRR. Gao et al. investigated and designed a planar inverted antenna design through metasurface, operated in the range of 4.9 to 5.9 GHz for WBAN applications. They designed the structure through the skin, fat, and muscle layers [36]. The 'S' shaped

Received 7 January 2022, Accepted 17 February 2022, Scheduled 18 March 2022

* Corresponding author: Srinivasan Ashok Kumar (ashokvaasan@gmail.com).

[1] Pondicherry University, Puducherry 605014, India. [2] Jyothishmathi Institute of Technology and Science, Karimnagar, India.

[3] Pondicherry Technological University, Puducherry 605014, India.

simple dual-mode microstrip antenna developed by Mendes and Peixeiro in 2018, it is operated in ISM band 2.45 GHz [4]. Kumar and Shanmuganantham [18], in 2020, designed a scalp-implantable antenna for biomedical applications. Kumar and Shanmuganantham [33], in 2020, reported a wide-band patch antenna with a compact CPW feeding network for L-band applications. The SRR can make the essential magnetic permeability negative medium to decrease the prototype size as well as designed monopole structure for 5G range from 3.4 to 3.6 GHz and WIFI 5.75 to 5.825 GHz bands, and it is useful for biomedical communication.

Waigh et al. [13] in 2019 designed "For body area networks with a versatile high-gain planar antenna, the versatile 2.4 GHz node". This antenna was designed through FR4 PCBs, and designed node passed through transmitter certification tests. A reported gain for a patch was −3.96 dB, for meandered −0.87 dB, and for dual ARM PIFA −7.04 dB, and all reported gains are negative. Hamouda et al. [15], in 2018, designed a double-band nano composite versatile antenna used for wearable biomedical applications. Here the negative gain of the antenna is −2.3 at 2.45 GHz. "CPW-fed slot antenna can be used for wearable medical devices." This antenna was designed through skin, fat, and muscles, layers and operated in ISM band (5.8 GHz) [22]. Metamaterial-inspired double SRR shaped antenna for medical application were designed. This antenna operated in 2.5 GHz. The gain was −6.8 dBi, and return loss was 23.95 dB [31]. Fig. 1 explains the working principle of a simple U slot antenna for networking system. The on-body sensors and antennas are placed on skin layers. The gathering of such antenna is a conversion of biomedical data (ECG signal) into electromagnetic waves, and at last, it reached into the medical center through the various networks [23]. The designed antenna is operated a limited band of frequencies, such as an ISM band (2.4 to 2.5) GHz and (3.4 to 3.6) GHz fifth-generation band.

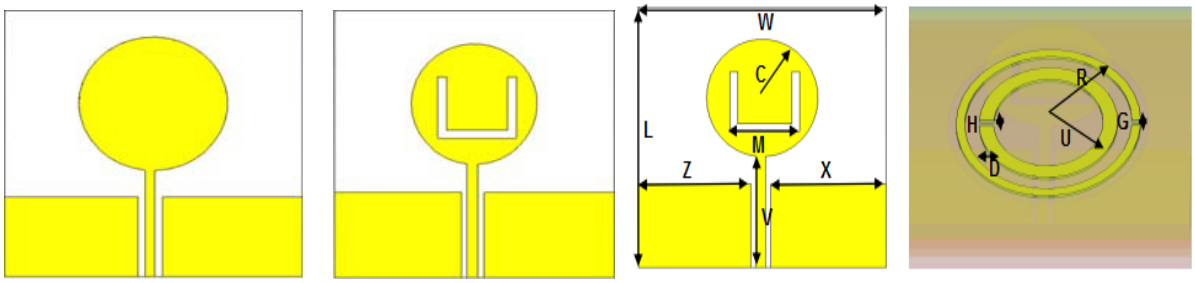

Figure 1. Antenna structure. (a) Circular shape. (b) U-slot antenna. (c) U slot. (d) Split ring resonator.

Section 1 discusses the theoretical concept of SRR loaded antennas for biomedical applications and also the various reported designs in the area of research. Section 2 involves the architecture of the proposed design and examines the dimensions. The modelling and discussion of various results are pointed out in Section 3. Finally, Section 4 is the conclusion part of this research work.

2. DESIGN AND DIMENSIONS

Two key elements are included in the proposed prototype model. The main parts comprise a grounded coplanar waveguide supplied with a U-slotted radiating structure loaded with a circular split ring resonator. Three biological surface layers, muscle layers, skin and fat, which are electromagnetic absorbed layers, are to be composed in the subsequent section. These layers are necessary for ECG monitoring [29]. The U-slotted antenna has a high compressive nature as compared to another slotted antenna. The defect grounded CPW with the SRR prototype model is established on the apex of the skin or below the substrate. The U-slot structure is created by etching of copper material as shown in Fig. 2. Teflon is a biocompatible substrate material used for the design of the proposed antenna. The Young's module of Teflon is 0.5 KN/mm^2, and dielectric permittivity is 2.1 [18, 19]. Two significant technologies are used in the developed antennas. The first method is CB-CPW fed; it

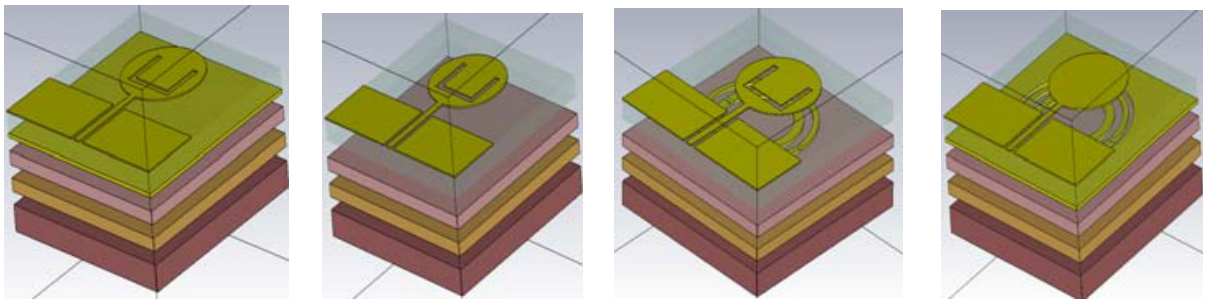

(a) (b) (c) (d)

Figure 2. Antenna simulation setup model. (a) CBCPW. (b) CPW. (c) CPW fed U-slot. (d) SRR loaded CBCPW.

has low attenuation characteristics and dispersion. The subsequent method has metamaterial loaded using SRR loaded technology. The main characteristics of SRR loaded configurations are easy to tune the desired frequencies, to have gain enhancement, bandwidth improvement, and multibands, and miniaturization [21, 30].

The designed steps involved in the proposed antenna are given in Fig. 4, Fig. 5, Fig. 6, and Fig. 7. First, we design the CB-CPW fed circular patch structure. The various types of feeding mechanisms with and without the presence of SRR loaded proposed prototype model have been analyzed through simulation, and their results are obtained and plotted in Fig. 9 to Fig. 11. Fig. 1 indicates the dimensions of proposed antennas; the overall volume of the antenna is 640 mm^3. The length, width, and thickness of the antenna are represented in terms of wavelength $0.167\lambda_0$, $0.167\lambda_0$, and $0.013\lambda_0$. Table 1 indicates the values of dimensional parameters. Table 4 indicates the comparison results of the developed prototype and various literature papers.

Table 1. The dimensions for U slot antenna.

Size	Unit (mm)	Size	Unit (mm)
L	20	U	2.6
W	20	H	0.5
Z	7.2	G	0.5
X	7	M	6.4
C	6.6	V	4.6
R	3.8	D	1

3. EXPERIMENT AND EQUIVALENT CIRCUIT

Figure 3 indicates the equivalent circuit model for SRR of the design and development of the prototype model. The first stage indicated the requirements and specifications of the prototype model for ECG monitor applications. The most important characteristic required for a medical device is low noise behaviour. Since the first stage of design, we used biocompatible dielectric substrate material with low loss; loss tangent value-Teflon is the best option. CPW feed has dispersion and attenuation characteristics. The electrical strength of the skin layer in human tissue at 2.45 GHz is $\epsilon_r = 52.79$ and reciprocal resistivity of 0.71 (s/m) at 2045 GHz [Tables 2 & 3]. The prototype bio-tissue is located in the middle of an artificial box of the volume $20 \times 20 \times 8$ cm filled with 1000 ml of liquid phantom. The nonconductive description of fat, skin, tissue, and human muscle is imitated by this liquid at 2.45 GHz and 3.5 GHz and prepared based on Table 3. If the measured values and their physical interpretation are

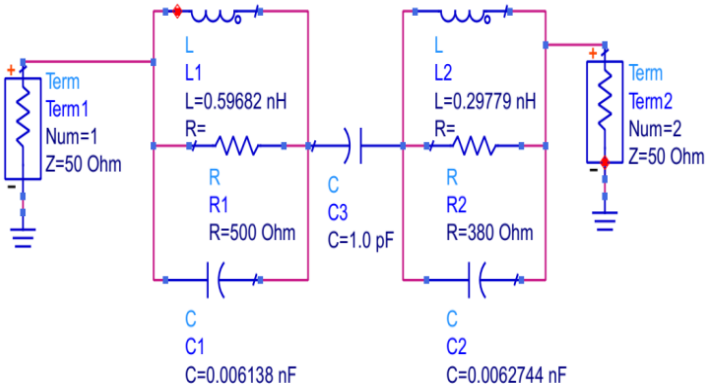

Figure 3. Approximated equivalent circuit model of SRR structure.

Table 2. The bio-tissues layer thickness of proposed prototype.

Human tissue	Size
Antenna substrate	1.6 mm
Skin	1 mm
Fat	3 mm
Muscle	40 mm

Table 3. Dielectric values (avg. value) for human tissues at 2.45 GHz.

Bio-layers	Electric permittivity	Conductivity	Loss Tangent
Skin	$\varepsilon_r = 38$	Sigma = 1.46	0.55
Fat	$\varepsilon_r = 5.28$	Sigma = 0.11	0.33
Muscle	$\varepsilon_r = 52.79$	Sigma = 1.71	0.24

acceptable for our objective of the research, then the process will stop, otherwise, redesign and continue. The RLC equivalent circuit representation of SRR and proposed antenna are shown in Fig. 3. The first circuit generates a 2.45 GHz operating frequency, and another circuit generates a 3.5 GHz operating frequency. The RLC equivalent representation has been realized by using ADS software, and S_{11} and VSWR parameters are obtained from CST MWS. The mathematical equation of R, L, C is given below

$$R = 2Z_o \left[\frac{1}{|S_{11}|^2} - 1\right] \Omega$$

$$C = \frac{0.25 f_{cs}}{\pi \left(f_{op}^2 - f_{cs}^2\right)} \text{nF}$$

$$L = \frac{1}{4\pi^2 f_{cs}^2 C} \text{nH}$$

4. RESULTS & DISCUSSION

In the present circumstances, the antenna is designed to place on the surface of the bio-tissues, and subcutaneously, it is mainly attached to the skin, fat, and muscle tissues [1]. In measurement instance, the antenna under test is placed on the skin layer surface of the right hand fabricated U-slot shape and SRR structure as shown in Fig. 4. The prototype is found at the center of a synthetic box of the

Figure 4. Low profile fabricated antenna on the surface of left-hand.

volume $20 \times 20 \times 8$ cm filled with 1000 ml of phantom solution. The phantom's solution represents the nonconductive description of body muscle, fat, and skin layers at 3.5 GHz and 2.45 GHz; otherwise, the prototype is directly tested on hand, shown in Fig. 4. The reflection coefficients and return loss are shown in Figs. 5 and 6. An antenna's bandwidth is derived from either the VSWR plot or return loss. The VSWR values are trustily obtained from the reflection coefficient plot [11]. The measurement of on-body antenna is little bit difficult because of the wide range of variation in dielectric constant values of bio-tissues. Moreover, the human body is treated as anisotropic behavioural characteristics. The feed is used to connect the prototype, then connected to the vector analyzer which might provide measurements.

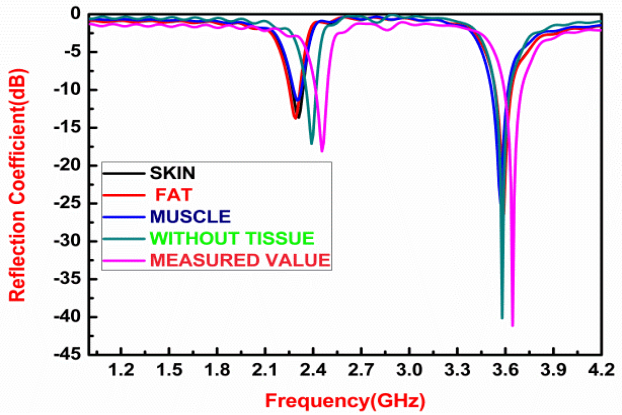

Figure 5. Reflection coefficient plot for U-slot with CBCPW fed antenna.

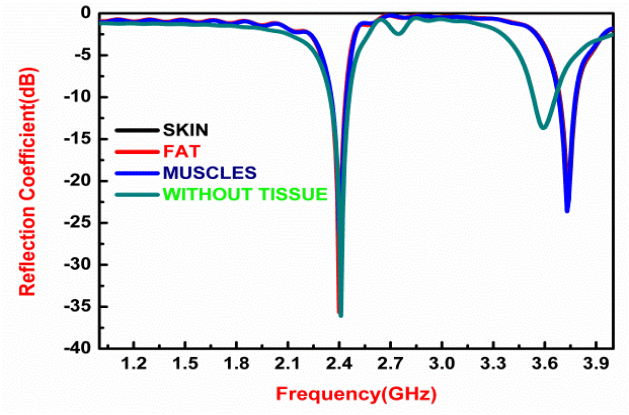

Figure 6. Reflection coefficient plot for circular antenna with CBCPW fed.

4.1. Prototype Analysis On-Body Model

In the core, we prepared an ordinary human phantom solution for the body form with properties including relative epsilon value 52.7 and conductivity 1.71 S/m at 2.45 GHz, and for 3.5 GHz, the relative epsilon value 49.6 and conductivity 1.52 s/m. Subsequently, the human tissues structures were utilized to mimic solution. The parametric values of radiated energy absorbed by tissues were acquired from the library documentation in CST MWS. The SRR loaded AUT, no SRR with CB-CPW feed, FS and on-body models, and phantom models are presented.

Based on the fifth generation medical service band and industrial science and medical band, the proposed design has been operated [2, 33]. As a double-band antenna, based on the reflection coefficient

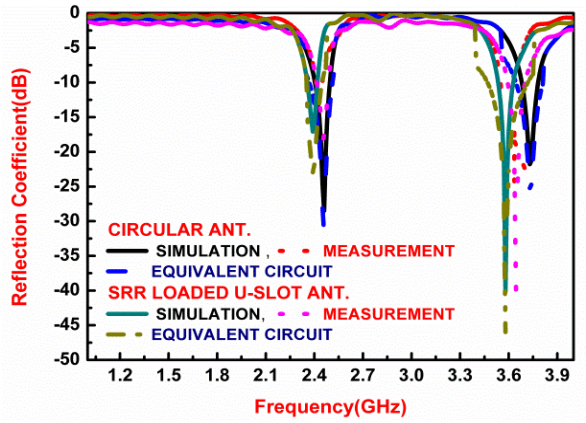

Figure 7. S_{11} results of circular and U-slot antenna with SRR loaded.

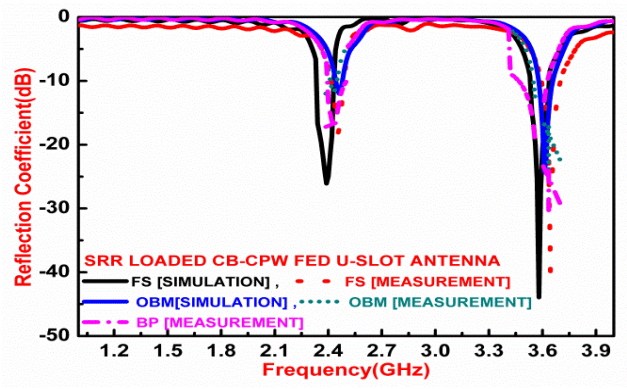

Figure 8. S_{11} plot for FS, OBM and BP of U-slot antenna with SRR.

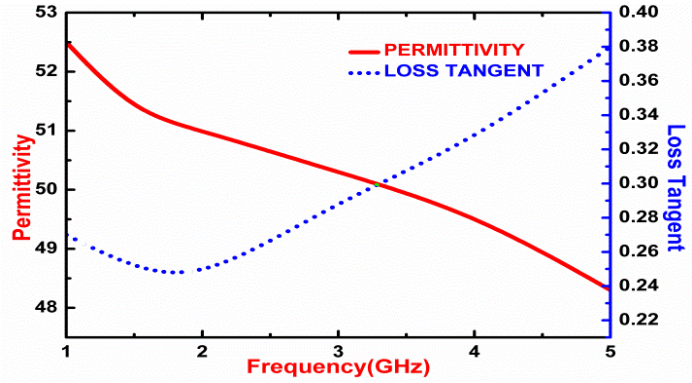

Figure 9. Dielectric constant measurement.

plot, bandwidth has been calculated. The decibel values of S_{11} are: -28 dB in 2.45 GHz, -24 dB in 3.55 GHz intended for a circular patch. Values are -38 dB in 2.42 GHz and -24 dB in 3.6 GHz designed for a U-slot antenna without the use of SRR loaded technique. -18 dB in 2.41 GHz, -41 dB at 3.5 GHz with the use of U-slot SRR loaded antennas are shown in Fig. 7 and Fig. 8, respectively. There is a clear fact that when we loaded body models into the planar configured antenna, the antenna gain has been detuned towards lower frequencies. This electromagnetic absorption layers (body tissue) lead to the more dispersive or attenuate nature of the antenna, hence on-body antenna produced a negative gain characteristic property.

On the other hand, the SRR U slot antenna is non slot with a very simple structure. The antenna is simulated on a three layered body model and FS. The reflection coefficient values are -30 dB for (simulation), -15 dB (measurement), -32 dB (equivalent circuit model) at 2.45 GHz, -40 dB for (simulation), -23 dB (measurement), -44 dB (equivalent circuit model) at 3.5 GHz for circular patch. Reflection coefficient values are SRR loaded U-slot -25 dB for (simulation), -18 dB (measurement), -26 dB (equivalent circuit model) at 2.45 GHz, -43 dB for (simulation), -37 dB (measurement), and -46 dB (equivalent circuit model) at 3.5 GHz for U-slotted patch.

The majority of metamaterials used in general are based on double split-ring resonators (SRRs) and split ring resonator which shows negative permeability. The magnetic dipole is caused by ring splits and the distance between the inner and outer rings. Due to a parallel, identical, and time-varying magnetic field produced current flows in two rings, but opposite directions. The equivalent circuit model is shown in Fig. 3. The model of this circuit is identical to an oscillating LC circuit, so the device functions as an LC resonator [9, 10, 12]. It could be shown at the resonance that the present flow path is opposite at

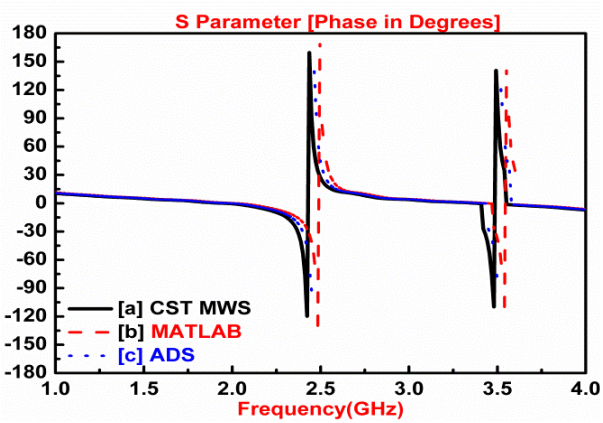

Figure 10. Positive and negative phase responses of SRR.

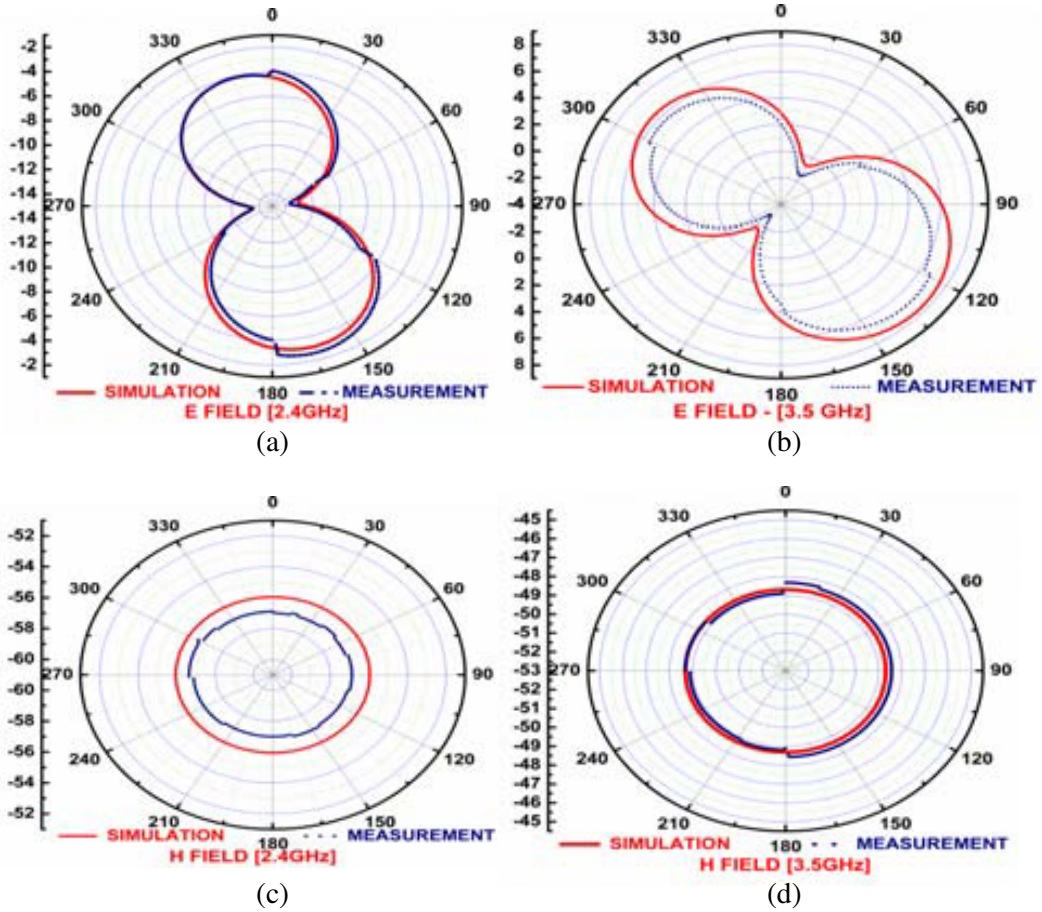

Figure 11. Radiation pattern (a) E-plane at 2.4 GHz, (b) E-plane at 3.5 GHz, (c) H-plane at 2.4 GHz, (d) H-plane at 3.5 GHz.

the resonance splits. Fig. 10 shows a negative permittivity parameter in terms of phase and frequencies. The first resonance phase change has happened at 2.45 GHz and the second resonance phase change at 3.5 GHz, and this change plot is based on MATLAB software, equivalent circuit model, and CST simulated results.

In this paper, the standing wave ratio indicates impedance corresponding to the property of the phantom model, built on-body model and FS model. The planned antenna values for a circle-shaped

antenna are 1.03 in 2.45 GHz and 1.11 in 3.5 GHz. The U-slot with 1.001 in 2.45 GHz and 1.13 in 3.5 GHz with no SRR loaded antenna is depicted, and measurement result is 1.08 in 2.45 GHz and 1.28 in 3.6 GHz for circular form with SRR loaded CBCPW feed, 1.2 in 2.45 GHz and 1.3 in 3.5 GHz for U-slot without SRR loaded antenna, and 1.2 in 2.43 GHz and 1.08 in 3.6 GHz for U-slot SRR loaded antenna.

The radiation pattern of U slot patch antenna shows unique characteristics. The field pattern is classified as field pattern (H-plane pattern) and an electric field pattern (E-plane). Fig. 11 displays the U-slot patch antenna polar plots of far-field E and H fields. The maximum electric fields point to broadside direction at 2.45 GHz, but in the case of 3.5 GHz tilted some solid angle (approximately 25 degree) because of the operated higher frequency, the phase changes due to the coupling effect between the radiating structure and split ring resonator. This radiation pattern characteristic is similar to the omnidirectional radiation pattern characteristics. Fig. 12 shows the gain maximum or directivity of the proposed prototype model. The patterns of directivity are close to the pattern of grounded dipole antenna radiation.

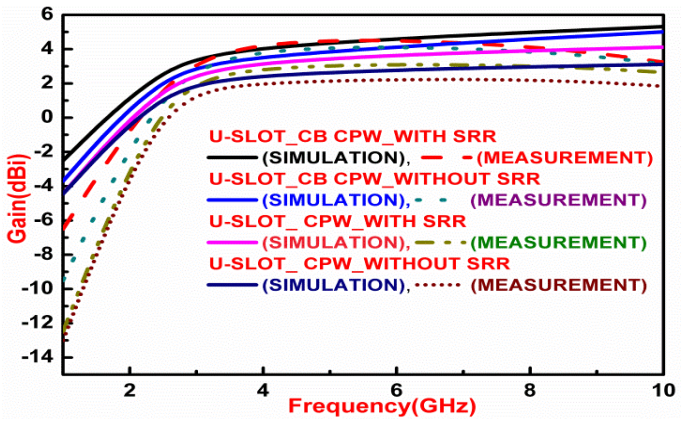

Figure 12. Characteristics of gain over frequency.

Table 4. Comparisons between referred antennas and proposed antennas.

Referred papers	Size [mm^3]	Gain [dBi]	BW [MHz]
[25] S. Fernandez et al.	1524	−16	12
[26] T. Karacolak et al.	1265	−25	142
[27] C. M. Lee et al.	790	−27	120
[13] M. Waigh et al.	896	−10	150
[15] Z. Hamouda et al.	302	−2.3	120
[16] M. Rizwan	4212	−10	480
[17] B. Y. Akowash	2284	3.1	–
SRR-CBCPW fed Circular, $f = 2.45$ GHz	640	3.3	128
SRR-CBCPW fed Circular, $f = 3.6$ GHz	640	4.7	112
CBCPW fed U-slot $f = 2.4$ GHz	640	2.5	152
CBCPW fed U-slot $f = 3.6$ GHz	640	4.3	130
SRR-CBCPW fed U-slot $f = 2.41$ GHz	640	2.9	146
SRR-CBCPW fed U-slot $f = 3.6$ GHz	640	4.6	160

4.2. Prototype Performance on Free Space and Body Phantom

The field pattern is measured in an anechoic chamber, from the advance research Thiagarajar center/Thiagarajar telecom solution limited (TTSL) in Madurai, India. The antenna placed inside the anechoic chamber is given in Fig. 13. The FS impedance of an antenna is greater than the on-body model and body liquid phantom mimic solution. The simulated impedance bandwidth of the proposed design in FS is 190 MHz at 2.45 GHz and 176 MHz at 3.5 GHz for U-slot with SRR. 185 MHz in 2.45 GHz and 169 MHz in 3.5 GHz for U-slots with a non-SRR loaded structure were simulated by the FS. For circle-shaped SRR loaded structures, the FS simulated results are 153 MHz in 2.45 GHz and 142 MHz in 3.5 GHz. On-body communication's standard band requirement is 1 MHz [32].

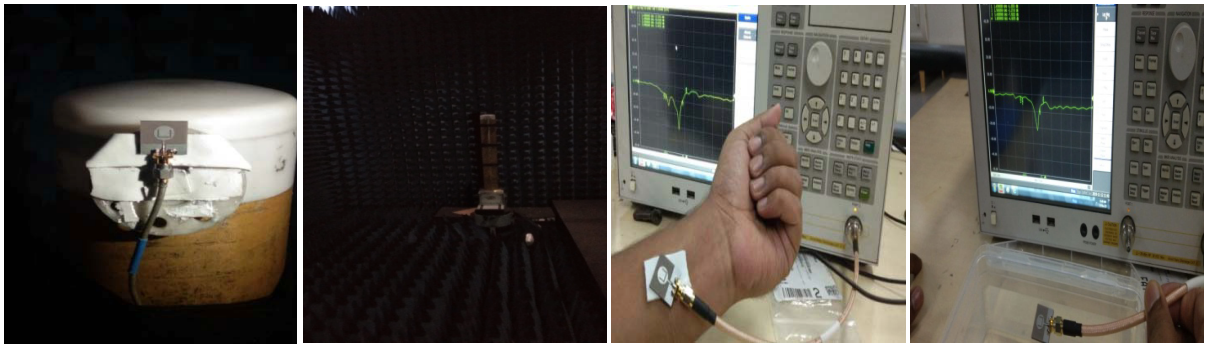

Figure 13. Antenna measurement did inside the anechoic chamber and VNA.

The prototype is found at the centre of a synthetic box of the volume which is $20 \times 20 \times 8$ cm packed with one litre of phantom liquid. The phantom planning details can be seen in [1, 24]. The tangent of loss angle of bio-tissues (skin, fat, and muscle) phantom and dielectric constant have been measured by the keysight vector network analyzer, with a range of frequency from 1 to 10 GHz, given in Fig. 13. The SRR loaded CB-CPW fed is able to preserve minimum of reflection coefficient when it is found on the muscle tissue phantom.

4.3. Antenna Evaluation: Surface Current and *E* & *H* Field

The electric and magnetic field curl gives the average electromagnetic power flow orientation per unit area or direction of the electromagnetic waves propagating. The curl of electric and magnetic field

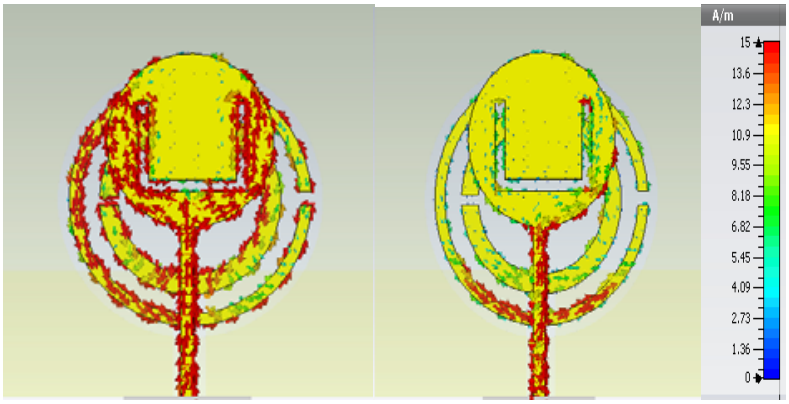

(a) (b)

Figure 14. Surface current distribution on proposed SRR loaded CBCPW.

vectors is called the Poynting vector, hence this theory is called as Poynting theorem. Figs. 15 and 16 show that an electric field is maximum where magnetic-field is minimum, and electromagnetic signal propagates through the perpendicular orientation of both electric field vector and magnetic field vector. The depth of penetration decreases inversely proportional to the square root of operating frequency, hence at a higher frequency, the SAR will be high and harmful for on-body application. The surface current distributions of the proposed antenna at 2.45 GHz and 3.5 GHz are given in Fig. 14, and the surface current unit is (A/m).

An antenna's input resistance is equal to the sum of the antenna's ohmic resistance and radiation resistance. The ohmic resistance is the summation of the conductor resistance and biological material resistance. The conductor resistance and biological material resistance are influenced by the counter current distribution of the designed prototype. At resonance, the antenna performs as an open circuit with large input impedance, and the input resistance of antenna decreases above and below the transition region. At this instant the ohmic losses are insignificant compared to the large radiation loss. It means that under resonance condition the AUT impedance is mostly controlled by radiation resistance.

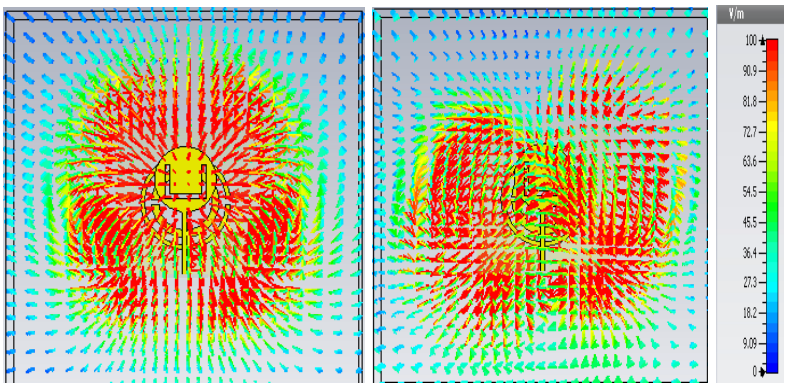

(a) (b)

Figure 15. *E*-far field distribution on proposed SRR loaded CBCPW.

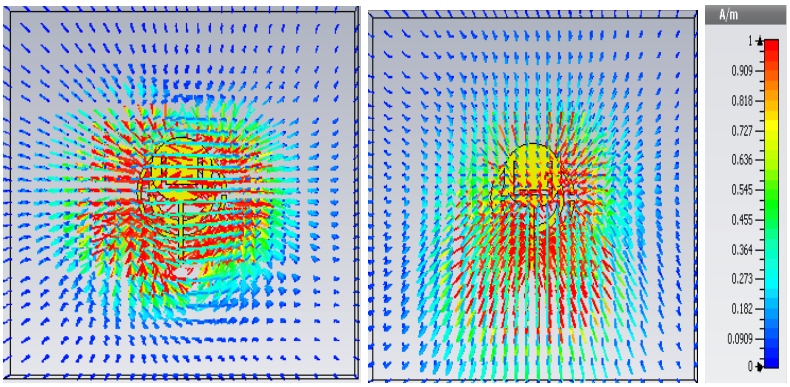

(a) (b)

Figure 16. *H*-far field distribution on proposed SRR loaded CBCPW.

4.4. Antenna Evaluation: Specific Absorption Rate

In the antenna under test, the SAR level of the on-body prototype should be validated to certify the compliance with safety limits. In addition, SAR is used to point out the health hazards posed to humans through on-body radiators. "According to the recommendations of IEEE C95.1-1999 [5]

and IEEE C95.1-2005 standards, electromagnetic energy which is absorbed by bio-tissues should not be greater than 1.6 W/kg for 1 g tissue or 2 W/kg for 10 g tissue." [6, 7]. Root mean square (RMS) electric field strength SAR is measured within the human body. Conductivity, density of mass, and dielectric constant are the important properties of bio-tissues. Based on the IEEE C95.1 standard, SAR is determined here using the mass average method calculated using CST software. The 1 W (RMS) was set as the input power to feed an antenna for the simulation of the SAR values [1]. Fig. 17 gives the measured SAR values, and summarized results is in Table 5. The SRR loaded without conductor backed CPW feed and SRR loaded U-slot with CBCPW feed are shown in Fig. 17. One of the important aspects from the SRR loaded U-slotted antennas is that SAR values are lower than that of safety limits. The SAR analysis signifies the preeminence of the SRR loaded CB-CPW fed antenna used for working close to the humans [8]. Hence, we concluded that SRR loaded CB-CPW fed antennas' SAR values are within regulated limits so that it will not be an issue for proposed low profile antennas and biocompatible for the future use of biomedical applications.

Table 5. Comparisons between various parametric results of proposed CBCPW feed antennas.

SL.No	Parameters	U-SLOT CB-CPW_WITH SRR				U-SLOT CB-CPW_WITHOUT SRR			
		2.45 GHz		3.5 GHz		2.45 GHz		3.5 GHz	
		Sim.	Mea.	Sim.	Mea.	Sim.	Mea.	Sim.	Mea.
1	Dimension	20 mm × 20 mm × 1.6 mm				20 mm × 20 mm × 1.6 mm			
2	Substrate	PTFE_Teflon [Epsilon 2.1]				PTFE_Teflon [Epsilon 2.1]			
3	Feeding technique	CB-CPW				CB-CPW			
5	Reflection coefficient [dB]	−25	−18	−43	−37	−35	−29	−24	−17
6	Impedance matching	49.13	50.8	49.13	51.28	49.19	50.23	49.13	51.28
7	VSWR	1.18	1.26	1.08	1.12	1.01	1.17	1.13	1.24
8	Impedance bandwidth	6.2	9.1	3.7	5.3	2.9	3.3	2.9	3.6
9	Gain [dBi]	2.9	1.9	4.6	4	2.5	1.6	4.3	3.6
10	SAR value [W/kg]	0.067		0.337		0.253		0.623	
11	E plane_3 dB angular width [deg.]	87.6	83.1	105.2	100.3	89.2	95.3	106.7	112.3
12	H plane_3 dB angular width [deg.]	97.2	120.3	106.7	102.6	90.3	100.1	107.3	116.3

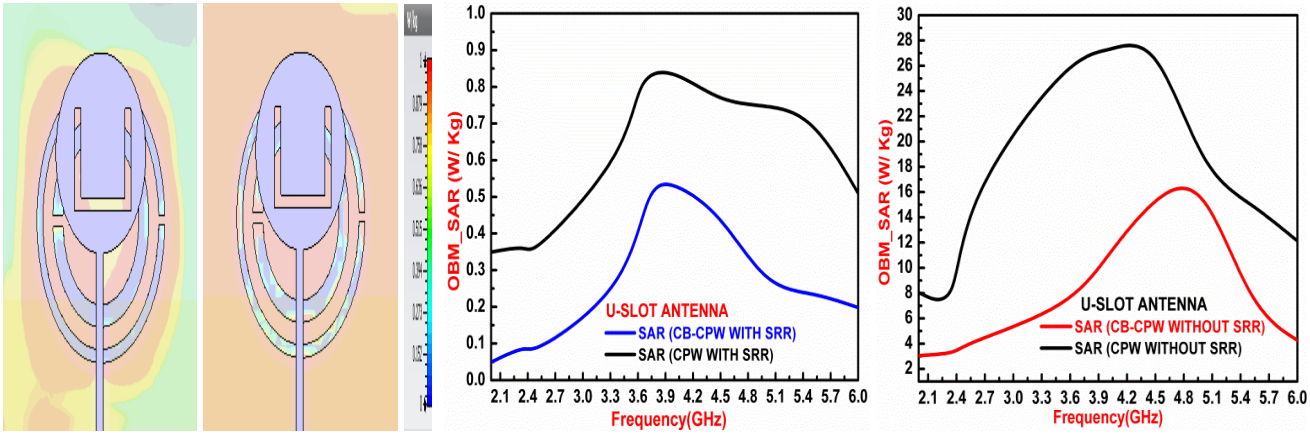

(a) (b) (c)

Figure 17. SAR distribution. (a) OBM 2D model. (b) SRR loaded U-slot with CBCPW feed. (c) SRR loaded without conductor backed CPW feed.

5. CONCLUSIONS

Under various conditions, a conductor-backed CPW-fed SRR loaded dual-band antenna has been designed and measured. The first resonance of the built prototype occurs at the ISM band, and the second resonance occurs at the fifth generation medical service band. The proposed prototype has a total size of 640 mm^3 (lower volume). In addition, the proposed system is metamaterial or SRR loaded with a conductor-backed CPW fed part, so that the traditional antennas have a lower dispersion and attenuation value. The proposed prototype model has been configured with muscle layers, skin, and fat, and it has been used to monitor ECG and also for various applications related to healthcare.

REFERENCES

1. Alemaryeen, A. and S. Noghanian, "On-body low-profile textile antenna with artificial magnetic conductor," *IEEE Transactions on Antennas and Propagation*, Vol. 67, No. 6, 3649–3656, Jun. 2019.
2. Sajith, K., J. Gandhimohan, and T. Shanmuganantham, "Design of conductor backed coplanar wave guide fed split ring resonator loaded loop antenna for on-body electrocardiography monitoring applications," *Journal of Computational and Theoretical Nanoscience*, Vol. 16, 1344–1349, 2019.
3. Gao, G.-P., C. Yang, and B. Hu, "A wearable PIFA with an all-textile metasurface for 5 GHz WBAN applications," *IEEE Antennas and Wireless Propagation Letters*, Vol. 18, No. 2, 288–292, Feb. 2019.
4. Mendes, C. and C. Peixeiro, "On-body transmission performance of a novel dual-mode wearable microstrip antenna," *IEEE Transactions on Antennas and Propagation*, Vol. 66, No. 9, 4872–4877, Sep. 2018.
5. Test plan for wireless device over-the-air performance, revision 3.5.2, CTI certification standard, Olympia, WA, USA, Sep. 2015.
6. IEEE Recommend Practice for measurements and computations of radio frequency electromagnetic field with respect to human exposure to such field, 100 kHz–300 GHz, standard IEEE C95.3-2002, 2002.
7. Council Recommendation on limits for exposure of the federal public to electromagnetic field: 0 Hz–300 GHz, commission of European Communities, 1988.
8. Arif, A., M. Zubair, M. Ali, M. U. Khan, and M. Q. Mehmood, "A compact, low-profile fractal antenna for wearable on-body WBAN application," *IEEE Antennas and Wireless Propagation Letters*, Vol. 18, No. 5, 981–985, May 2019.
9. Kumar, S. A. and T. Shanmuganantham, "Design of bending antennas for purpose of biomedical applications using novel approach," *Transaction on Electricals and Electronic Materials*, Springer, Feb. 2021.
10. Engheta, N. and R. W. Ziolkowski, *Metamaterials Physics and Engineering Explorations*, John Wiley & Sons, 2006.
11. Balanis, C. A., *Antenna Theory Analysis and Design*, 4th Edition, John Wiley & Sons, 2016.
12. Itoh, T. and C. Caloz, *Electromagnetic Metamaterials Transmission Line Theory and Microwave Applications*, John Wiley & Sons, 2006.
13. Waigh, M., Y. Wew, and S. Beeby, "Flexible 2.4 GHz node for body area networks with a compact high-gain planar antenna," *IEEE Antennas and Wireless Propagation Letters*, Vol. 18, No. 1, 49–53, Jun. 2019.
14. Ali, K., A. Hasanvand, and I. Balasigham, "Radio frequency backscatter communication for high data rate deep implants," *IEEE Transactions on Microwave Theory and Technique*, Vol. 67, No. 3, 1093–1106, Mar. 2019.
15. Hamouda, Z., J. L. Wojkiewicz, A. P. Alexander, L. Kore, S. Bergheul, and T. Laseri, "Magnetic nanocomposite polymer-based dual-band flexible antenna for wearable application," *IEEE Transactions on Antennas and Propagation*, Vol. 66, No. 7, 3271–3277, Jul. 2018.

16. Rizwan, M., U. Leena, and J. Uirkki, "Flexible and stretchable brush-painted wearable antenna on a three-dimension (3D) printed substrate," *IEEE Antennas and Wireless Propagation Letters*, Vol. 16, 3018–3112, Oct. 2017.
17. Akowash, B. Y., P. Kosmas, and Y. Chen, "A Q-slot monopole for UWB body-centric wireless communication," *IEEE Transactions on Antennas and Propagation*, Vol. 65, No. 10, 5069–5075, Oct. 2017.
18. Kumar, S. A. and T. Shanmuganantham, "Scalp-implantable antenna for biomedical applications," *IEEE URSI Asia Pacific Radio Science Conference 2020 (AP-RASC 2020)*, Indian Institute of Technology Varanasi (BHU), Varanasi, Feb. 12–14, 2020.
19. Shanmugananthem, T., "Design and performance of implantable CPW fed Apollian shaped antenna at 2.45 ISM band for bio-medical applications," *Transaction on Electrical and Electronic Material*, Vol. 16, 250–253, Oct. 2015.
20. Braham, T. G., "Reference security architecture for body area networks in healthcare applications," *International Conference on Platform Technology and Service*, 2018.
21. Kumar, S. A. and T. Shanmuganantham, "Design and analysis of implantable CPW fed bowtie antenna for ISM band applications," *AEU: International Journal of Electronics and Communication*, Vol. 68, No. 2, 158–165, Elsevier, Feb. 2014.
22. Fernandez, S. and T. Quvendo, "Dual band microstrip patch antenna based on short circuital ring and spiral resonator for implantable medical device," *IET Microwaves, Antennas and Propagation*, Vol. 4, No. 8, 1048–1055, Apr. 2010.
23. Karacolak, T. and Hood, "Design of dual band implantable antenna and development of skin mimicking gels for continuous glucose monitoring," *IEEE Transactions on Microwave Theory and Technique*, Vol. 56, No. 4, 1001–1008, Sep. 2008.
24. Narmadha, G., M. Malathi, S. A. Kumar, T. Shanmuganantham, and S. Deivasigamani, "Performance of implantable antenna at ISM band characteristics for biomedical base," *ICT Express*, Elsevier, May 2021.
25. Kyriacou, E. and M. S. Pattichisn, "m-health e-emergency system: Current status and future directions," *IEEE Antennas and Propagation Magazine*, Vol. 49, No. 1, 216–231, Feb. 2007.
26. Shanmuganantham, T., B. Kumar, and S. A. Kumar, "Analysis of tree-shaped slotted impedance matching antenna for 60 GHz femtocell applications," *ICT Express*, Elsevier, Feb. 2021.
27. Elavarasi, C. and T. Shanmuganantham, "SRR loaded periwinkle flower shaped fractal antenna for multiband applications," *Microwave and Optical Technology Letters*, Vol. 59, 2518–2525, Oct. 2017.
28. Shanmuganatham, T., S. A. Kumar, and S. Selvi, "CSRR loaded CBCPW fed H-shaped slot radiator for ECG monitoring," *International Journal of Ultra Wideband Communications and Systems (IJUWBCS)*, Inderscience, Jul. 2021.
29. Morassaghi, S., M. Abolhasan, and J. Lipman, "Wireless body area networks: A survey," *IEEE Communication Surveys and Tutorial*, Vol. 16, No. 3, Third quarter, Mar. 2014.
30. Kumar, S. A. and T. Shanmuganantham, "Design of CPW-fed inverted six shaped antenna for IoT applications," *Transaction on Electricals and Electronic Materials*, Vol. 21, 524–527, Springer, 2020.
31. Kumar, S. A. and T. Shanmuganantham, "Design and performance of textile antenna for wearable applications," *Transaction on Electricals and Electronic Materials*, Vol. 19, No. 5, 352–355, Springer, Oct. 2018.
32. Srikanth, G., S. Ashok Kumar, and T. Shanmuganantham, "Design of ground radiation antenna by using compact EBG," *IEEE INDISCON 2020*, Visakapatnam, Oct. 2020, 10.1109/INDISCON50162.2020.00017.
33. Kumar, S. A. and T. Shanmuganantham, "Design of wideband patch antenna with compact CPW feeding network for L-band applications," *IEEE URSI Asia Pacific Radio Science Conference 2020 (AP-RASC 2020)*, Indian Institute of Technology Varanasi (BHU), Varanasi, Feb. 12–14, 2020.
34. Bose, J. C., "On the rotation of plane of polarisation of electric waves by a twisted structure," *Proceedings of the Royal Society*, Vol. 63, 389–400, 1898.

35. Veselago, V., L. Braginsky, V. Shklover, and C. Hafner, "Negative refractive index materials," *Journal of Computational and Theoretical Nanoscience*, Vol. 3. 189–218, 2006.
36. Gao, G., B. Hu, C. Yang, S. Wang, R. Zhang, "Design of a dual band-notched UWB antenna and improvement of the 5.5 GHz WLAN notched characteristic," *Journal of Electromagnetic Waves and Applications* Vol. 33, 1–12, 2019.